Computational simulation of the haemodialysis air trap

G. Keshavarzi, T. J. Barber, G. Yeoh, A. Simmons [1]

[1]School of mechanical and manufacturing engineering
University of New South Wales, New South Wales, Sydney, Australia

Abstract

Haemodialysis is an extracorporeal system used for blood filtration in renal disease patients. An important component of a haemodialysis system is the air trap, which is a safety feature to prevent any micro emboli and air from entering the body. Previously there has been clinical evidence of micro bubbles passing the air trap - this raises concern about the effectiveness of the air trap in capturing micro bubbles and micro emboli. The understanding of flow inside a haemodialysis air trap can help in the understanding of the motion and deposition of micro emboli. This paper presents numerical simulations of the flow structure of the air trap, allowing the investigation of the probability of the micro bubbles passing through the air trap. The results show the ineffectiveness of the air trap in capturing small sized micro bubbles, while only larger size bubbles were trapped.

Introduction

Kidneys are one of the major and complex organs in the body and are essentially the body's filter plant. Many diseases can cause renal failure which is when the kidneys fail to function. This is a very dangerous medical condition and needs to be treated. The Haemodialysis(HD) machine is widely used for end stage renal disease patients. While blood contaminations are being removed using the HD device it is believed that other impurities such as micro emboli both in gaseous and nongaseous states may be generated in the blood. This can result in dangerous long term health issues for the patient.

The HD device which acts as an artificial extracorporeal kidney contains 3 main parts (the blood pump, the membrane or dialyser, and air traps). The unclean blood is pumped from the patient arm artery, and through the dialyser's membrane which filters the blood using small membrane pores and a countercurrent flow of water. Before the blood is sent back to the patient through the fistula(an established connection between the vein and artery in the forearm theough surgery) in the patients arm, the device needs to make sure that there is no air going through the system. To prevent air from entering the body the safety feature used is an air trap and an air detector alarm is located at the end before injecting the cleaned blood back to the patient. In case the detector indicates air, the pump will stop working. The air trap has a height of about 15 cm and the blood level inside the air trap is adjustable,but the blood inside is usually recommended to be kept at a high level.

End stage renal disease (ESRD) patients suffer from medical issues in the long term. From many factors that might cause these condition, It was first noted in the 1970s one such factor is microembolization [1]. It was shown from in vitro studies that the origin of these microemboli is related to the HD device or blood lines because microembolism occurred only after the blood pump [2, 3]. Initially it was suggested that this could be due to platlet aggregations [4], but recent studies indicate that the microemboli are gaseous [5]. These microbubbles range in different sizes, and can have several side effects on the body. The chronic exposure of pulmonary vessels to microbubbles is likely to contribute to developing lung injury [2], and possibly a source of injury in the central nervous system(CNS); if the microbubbles cross from venous to systemic circulation they can also cause damage to the brain and other organs[6]. Cerebral atrophy[7], deterioration of neurocognitive functions[8], cardiovascular morbidity, and high mortality rates have also been recognised in HD patients [9] –the presence of microbubbles may be a main contributor.

Recently, the significance of microbubbles has been revisited, with the suspicion that air traps do not capture microbubbles and may even create them. The bubbles origination is currently unknown. In order to understand the effectivness of the airtrap, the flow inside the airtrap which affects the movement of the bubbles needs to be understood. In this paper, Computational Fluid Dynamics (CFD) has been used to model the blood flow in the air trap, to determine the flow structures inside the air trap which will control the flow of the bubbles. One of the difficulties in modelling an air trap is the free surface of the airtrap. Modelling the airtrap as a two fluid of blood and air using the two fluid models (VOF, Levelset, CLSVOF) is accompanied with restriction on the mesh element sizes. In order for the mesh elements to capture the microbubbles inside the air trap, several elements across each microbubble is required which makes modelling the entire airtrap computationaly expensive even in 2D. The flow inside the air trap has been investigated for two different models of the air trap showing the effect of the free surface and flow inside the air trap for a single and two fluid model.

Governing equations

The continuity and momentum equations for Newtonian, Incompressible flow formulation are given by:

$$\frac{\partial \rho}{\partial t} + \nabla \cdot \left(\rho V \right) = 0 \tag{1}$$

$$\rho(\frac{\partial v}{\partial t} + \mathrm{v} \cdot \nabla \mathrm{v}) = -\nabla p + \mu \nabla^2 \mathrm{v} + \mathbf{f} \tag{2}$$

Where ρ is the fluid density, v is the velocity, and μ the dynamic viscosity. The VOF model enables the capturing and tracking of the air-blood interface. An indicator function F ($0<F<1$) is used to indicate the presence of either the air or blood within each cell. The scalar advection equation for the indicator function F is solved according to the following:

$$\frac{\partial F}{\partial t} + \nabla \cdot \left(VF \right) = F \nabla \cdot \left(V \right) \tag{3}$$

The fluid properties – mixture density and viscosity – can be evaluated based on the linear dependence on the distribution of F as

$$\rho = \left(1 - F\right)\rho_{gas} + F\rho_{liquid} \quad (4)$$

$$\mu = \left(1 - F\right)\mu_{gas} + F\mu_{liquid} \quad (5)$$

In the VOF method Equation (3) is solved together with the conservation equation (1) and (2) to computational couple the velocity field and the volume fraction for each fluid. The appropriate evaluation of the fluxes across the element faces of the advection terms in equation (3) has been achieved by the geometric reconstruction based on the PLIC scheme.

Computational method and model

The ANSYS Fluent 12 software has been used to solve the flow of the blood in the air trap. The second order upwind scheme is applied for the spatial momentum discretization, and pressure staggering option (PRESTO) scheme was used for pressure discretization. To couple the pressure with the velocity in the incompressible limit, the coupled algorithm is employed.

The flow coming into the air trap is pumped through the HD device by a peristaltic pump which has a fluctuating velocity. The air trap has been modelled as a fluctuating sine wave inlet velocity with a time period of 6 seconds. The flow is considered incompressible, homogenous and Newtonian with a density and viscosity of 1058 kg/m^3 and 0.003 Pa.s. A fully structured mesh was developed for the region of the air trap. A time step of 0.001s was used for the flow. The inlet conditions were set as uniform across the boundary and fluctuating velocity in time. All cases were run with double-precision accuracy.

Two models of the air trap were modelled; one without the free surface and the other with the free surface of blood and air in the air trap (Figure 1). In Figure 1 the left model is the air trap modelled without the free surface, modelling the blood flow in the air trap. The right model in Figure 1 is modelling the free surface inside the air trap.
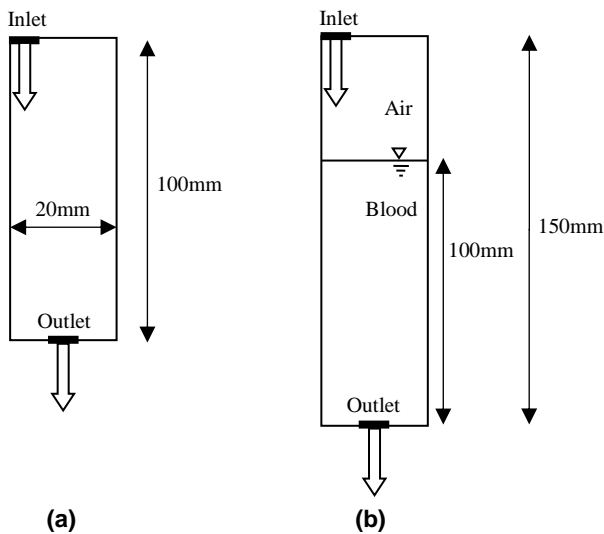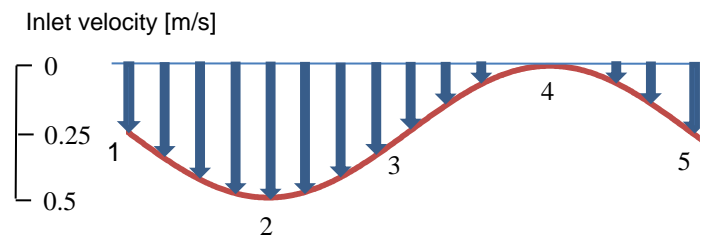
Results and discussion

The simulations in Figures 2 and 3 show the velocity and pressure contours at different times of the flow. The flow was simulated for 20 full cycles, allowing the flow properties to settle. The flow inside the air trap is shown to be very complex and rotational. For the air trap without a free surface at ¾ of the loop (point 4) where the velocity at the inlet is zero and the velocity starts to increase to a velocity of 0.5 m/s, there are 7 vortices: 4 of them are counter clockwise (CCW) and 3 are in the clockwise (CW) direction. With the increase of the inlet flow velocity the velocity stream strengthens the top vortex which is rotating in the CCW direction, and weakens the neighbouring vortex which is in the rotating CW. One second after the start of the inlet flow the bottom vortex which was the smallest in the other 7 vortices has been almost fully pushed out the air trap outlet and disappeared and only 6 vortices remains. Half a second after this at point 5 all the CW vortices have been damped out and only the 3 CCW ones remain as small vortices.

The two fluid model of the air trap is modelling the interaction of the blood with the air inside air trap resulting in air entrainment. The bubbles shown in Figure 4 indicate that there is air entrainment from the impact of the blood with the free surface in the air trap. While most of the big bubbles have a better chance of rising to the surface, Due to small buoyancy forces it is very unlikely for micro bubbles to rise to the free surface. The flow structure is also shown to be rotational similar to the previous one fluid model.

The vortices seen in both models generate low pressure areas within the flow. These low pressure zones are at the centre of the vortices, and due to the pressure gradient across the vortices bubbles and other micro emboli in these regions will be dragged towards the centre of these vortices; meaning the vortices have a significant effect on the bubbles distribution and flow inside the air trap. This can also be seen in Figure 4 with the bubbles being positioned in the centre of the vortices in the flow. The bigger the bubble the greater the pressure gradients drag across the vortex. Small size micro bubbles may or may not be influenced by the flow inside the air trap depending on the size range. Future studies on the buoyancy force and flow drag can show whether the air bubbles can be removed from the air trap.

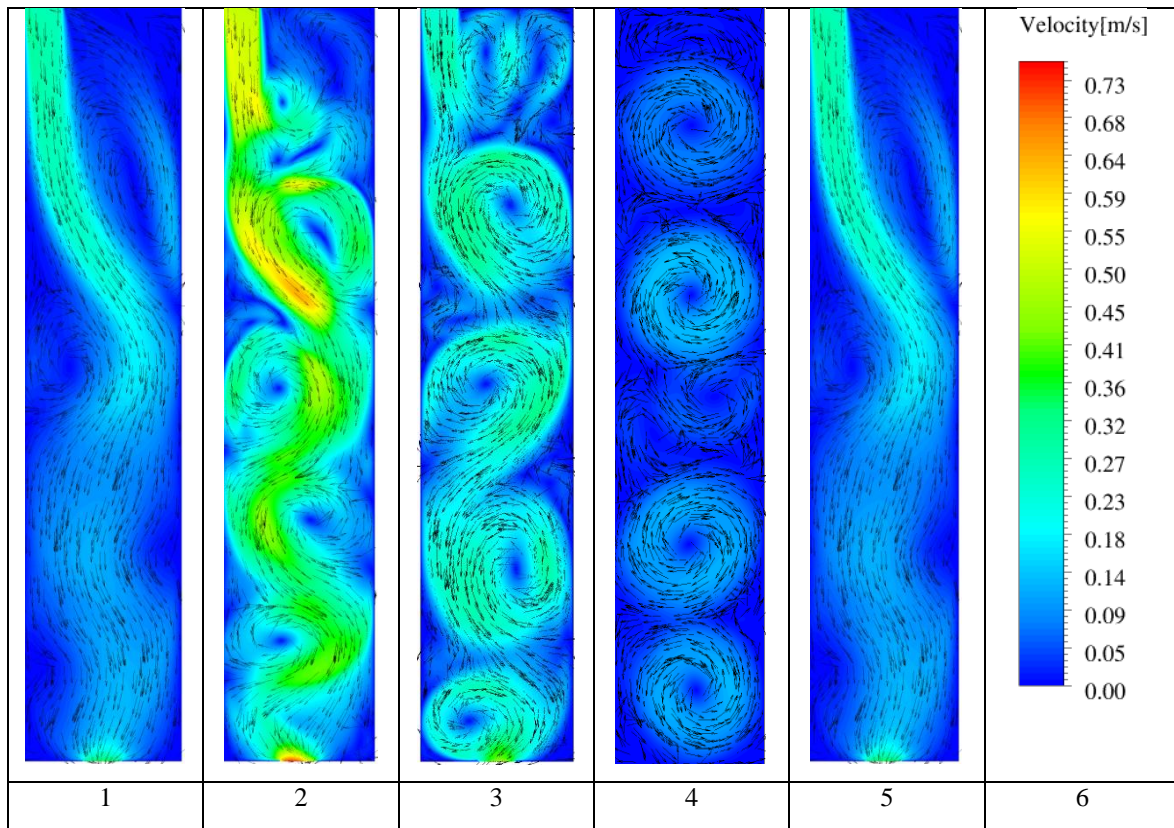Fig (1) – Two models of the air trap - (a)100mm without the free surface (b)150mm with 100mm free surface

Fig (2) – Instantaneous velocity contours of the blood flow inside the air trap at different times of the flow
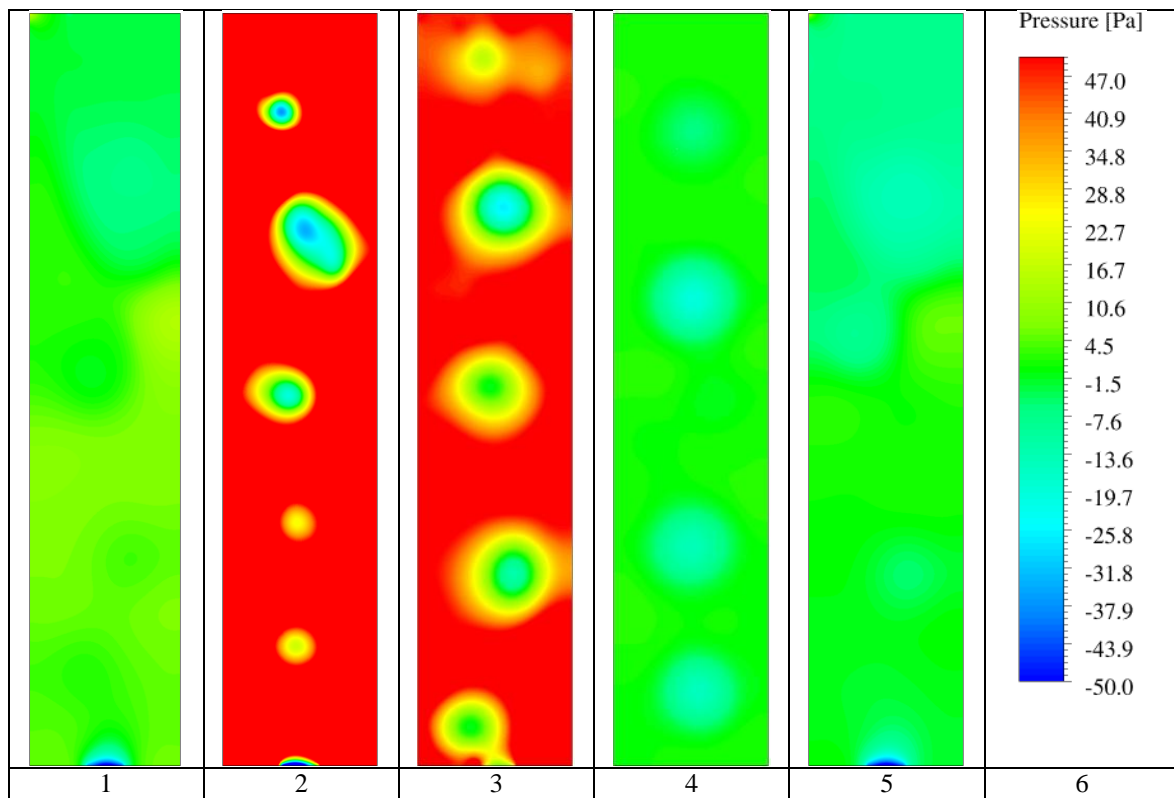

Fig (3)-Instantaneous pressure contours inside the air trap at different times of the flow
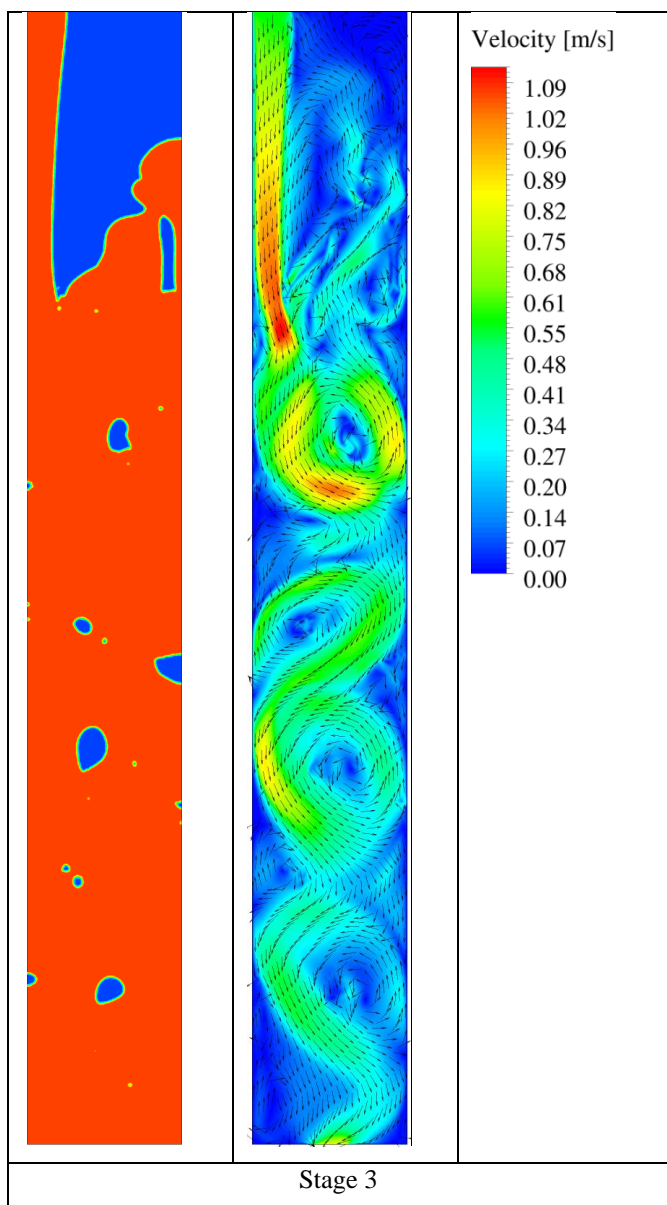
Fig (4) – Blood and with bubbles and velocity inside the 150 mm air trap (Fig (1b))

Conclusion

The modelling of the air trap has aimed to understand the flow inside the air trap. The two models used show the effect of the free surface in the flow field. It was shown from the rotational flow that the free surface of the air trap does not damp out the vortices in the flow, resulting in the presence of vortices in both models. These vortices generate low pressure regions inside the vortex which will drag the bubbles towards the centre of the vortex. Also major air entrainment from the impact of the blood with the free surface can be seen. Finally this paper has shown that not only the air trap is not removing bubbles it can also generate bubbles, and that the free surface air trap is an ineffective way of removing bubbles from the HD device.

References

1. Bischel, M.D., B.G. Scoles, and J.G. Mohler, *Evidence for pulmonary microembolization during hemodialysis.* CHEST Journal, 1975. **67**(3): p. 335-337.
2. Jonsson, P., et al., *Air Bubbles Pass the Security System of the Dialysis Device Without Alarming.* Artificial Organs, 2007. **31**(2): p. 132-139.
3. Rollé, F., et al., *Identification of microemboli during haemodialysis using Doppler ultrasound.* Nephrology Dialysis Transplantation, 2000. **15**(9): p. 1420-1424.
4. Ishii, Y., et al., *Evaluation of blood coagulation-fibrinolysis system in patients receiving chronic hemodialysis.* Nephron, 1996. **73**(3): p. 407-12.
5. Barak, M. and Y. Katz, *Microbubbles*Pathophysiology and Clinical Implications.* CHEST Journal, 2005. **128**(4): p. 2918-2932.
6. Barak, M., F. Nakhoul, and Y. Katz, *Reviews: Pathophysiology and Clinical Implications of Microbubbles during Hemodialysis.* Seminars in Dialysis, 2008. **21**(3): p. 232-238.
7. Savazzi, G.M., et al., *Progression of cerebral atrophy in patients on regular hemodialysis treatment: long-term follow-up with cerebral computed tomography.* Nephron, 1995. **69**(1): p. 29-33.
8. Pliskin, N.H., et al., *Neurocognitive function in chronic hemodialysis patients.* Kidney Int, 1996. **49**(5): p. 1435-40.
9. Schon, S., et al., *Renal replacement therapy in Sweden.* Scand J Urol Nephrol, 2004. **38**(4): p. 332-9.